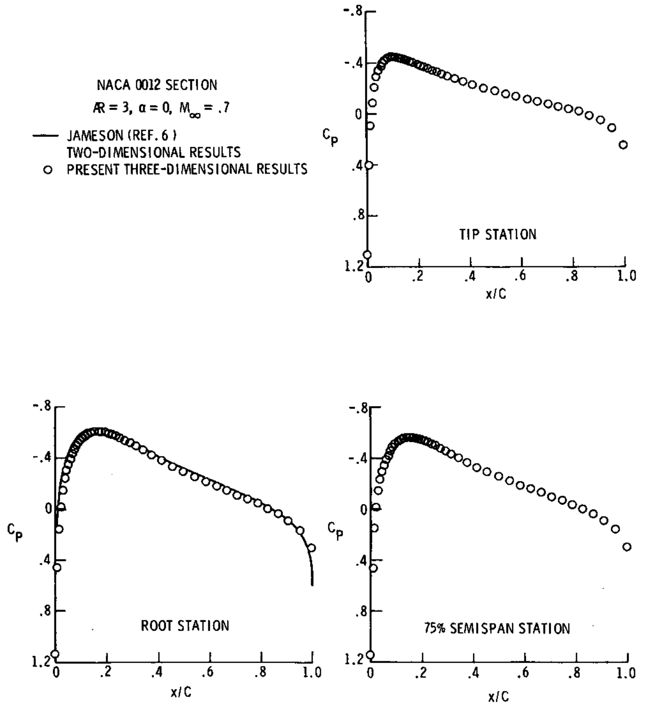

Fig. 2 Computed surface pressure coefficients for subcritical nonlifting rectangular wing with blunt leading edge.

required for similar computations with streamwise sweep only.

A comparison is made in Fig. 1 between the surface pressure coefficients obtained using the present method and those of Bailey and Steger.[7] These results are for a rectangular wing of aspect ratio 4 with a 6% thick biconvex airfoil section at 1° angle of attack and a freestream Mach number of 0.857. The value of critical pressure shown (C_p*) corresponds to the condition where the coefficient of ϕ_{xx} in Eq. (1) vanishes and, consequently, differs from the exact value. Agreement at the root and 60% spanwise station is very good; the differences in the region of the shock on the upper surface can be attributed to a greater resolution of the present results. Larger differences occur at the tip station and it should be noted that the loading does not vanish there for either solution. In the present computations, this tip station was treated the same as the other wing stations: that is, a zero load condition was not imposed at the tip. A nonzero load there implies that the wing tip is, in effect, between grid points; thus there is an uncertainty regarding the wing span. At the present stage of development, it is not clear how the tip region should be treated or how important the tip singularity is to the global flowfield solution. The computational mesh used for the present calculations shown in Fig. 1 contained $60 \times 22 \times 40$ grid points in the x, y, and z directions, respectively. There were 37 grid points on the airfoil at each spanwise station with 11 stations on the wing semispan.

Results of a subcritical ($M_\infty = 0.7$) three-dimensional calculation for a wing with a blunt leading edge at zero lift are shown in Fig. 2. The wing planform is again rectangular with an aspect ratio of 3, and the airfoil section is the NACA 0012. The pressure distribution at the wing root is compared with the very refined two-dimensional calculations of Jameson[6]; the agreement is quite good, although the very rapid expansion at the leading edge is not fully obtained in the three-dimensional computation. This is due in part to an insufficient number of grid points very near the leading edge. Similar computations for the same three-dimensional wing at lift and in supercritical flows showed much larger discrepancies in the leading-edge region using the same computational mesh. A successful computation for a blunt airfoil with the small disturbance equations requires that several grid points be located in the leading-edge region where the slope is large, and lack of such resolution causes errors in the rapid expansion in the leading-edge region and gives only a qualitatively correct behavior elsewhere.

The computations shown in Fig. 2 used a grid of $85 \times 20 \times 40$ in the x, y, and z directions, respectively, and required 300 K octal machine storage. Forty-eight of the 85 were located on the wing at each of 14 spanwise stations. A total of 85 grid points in the streamwise direction appears adequate for blunt airfoil computations; however, a larger percentage of them should be located on the wing with a higher density in the leading-edge region. Location of individual grid points to achieve a high density in the leading-edge region without excessively large higher derivatives in the coordinate transformation has proved difficult. However, these difficulties are computational in nature and are not inherent to the relaxation techniques or to the small-disturbance equations. It appears entirely feasible to calculate supercritical flows about wings of simple shape with blunt airfoil sections on present generation computers.

References

[1] Murman, E. M. and Cole, J. D., "Calculation of Plane Steady Transonic Flows," *AIAA Journal*, Vol. 9, No. 1, Jan. 1971, pp. 114–121.

[2] Murman, E. M. and Krupp, J. A., "Solution of the Transonic Potential Equation Using a Mixed Finite Difference System," *Proceedings of the 2nd International Conference on Numerical Methods in Fluid Dynamics*, Springer-Verlag, 1971, pp. 199–206.

[3] Krupp, J. A.and Murman, E. M., "The Numerical Calculation of Steady Transonic Flows Past Thin Lifting Airfoils and Slender Bodies," AIAA Paper 71-566, Palo Alto, Calif., 1971.

[4] Garabedian, P. R. and Korn, D. G., "Analysis of Transonic Airfoils," *Communications on Pure and Applied Mathematics*, Vol. 24, No. 6, Nov. 1971, pp. 841–851.

[5] Steger, J. L. and Lomax, H., "Transonic Flow About Two-Dimensional Airfoils by Relaxation Procedures," *AIAA Journal*, Vol. 10, No. 1, Jan. 1972, pp. 49–54.

[6] Jameson, A., "Transonic Flow Calculations for Airfoils and Bodies of Revolution," Aero. Rept. 390-71-1 (undated), Grumman Aerospace Corp., Bethpage, N.Y.

[7] Bailey, F. R. and Steger, J. L., "Relaxation Techniques for Three-Dimensional Transonic Flow About Wings," AIAA Paper 72-189, San Diego, Calif., 1972.

[8] Klunker, E. B., "Contribution to Methods for Calculating the Flow About Thin Lifting Wings at Transonic Speeds—Analytic Expressions for the Far Field," TN D-6530, 1971, NASA.

Eigenvalues and Eigenvectors for Solutions to the Radiative Transport Equation

J. A. Roux,* D. C. Todd,† and A. M. Smith‡
ARO Inc., Arnold Air Force Station, Tenn.

Introduction

THE transport equation for isotropic axisymmetric radiative transfer has the form

$$\frac{dI}{d\tau}(\tau,\mu) = \frac{-I(\tau,\mu)}{\mu} + \frac{W}{2\mu}\int_{-1}^{1} I(\tau,\mu')\,d\mu' + \frac{(1-W)}{\mu} n^2 I_b(T) \qquad (1)$$

Received February 28, 1972. This research was sponsored by the Arnold Engineering Development Center, Air Force Systems Command, under Contract F40600-69-C-0001 with ARO Inc.

Index categories: Radiation and Radiative Heat Transfer; Atmospheric, Space, and Oceanographic Sciences.

* Research Assistant; presently Senior Engineer, Northrop Services Inc., Huntsville, Ala.

† Mathematician, Central Computer Operations.

‡ Supervisor, Research Section, Aerospace Division, von Kármán Gas Dynamics Facility; also Associate Professor of Aerospace Engineering (Part-time), University of Tennessee Space Institute, Tullahoma, Tenn. Member AIAA.

where W = albedo, τ = optical thickness, $\mu = \cos\theta$, n = refractive index, $I_b(T)$ = Planck's intensity function, and I = radiative intensity. One standard method of solution has been the method of discrete ordinates whereby the integral term is approximated by a Gaussian quadrature.[1-3] This generates a system of simultaneous linear ordinary differential equations and the last term of Eq. (1) requires a particular solution. The method of solution of the homogeneous system of equations has been to numerically calculate the eigenvalues and eigenvectors. Much of the effort expended in obtaining a solution is therefore consumed in the computation of the eigenvalues and eigenvectors. Thus, a simple technique for finding the eigenvalues and eigenvectors would reduce the amount of work required in solving the homogeneous system of differential equations.

Most of the solutions presented previously have been for low to moderate albedo values.[4] If for high albedo values complex eigenvalues and eigenvectors were present, this would complicate the solution of the transport equation and also complicate the computation of the integration constants through use of the boundary conditions. Thus, it would be of value to know the nature of the eigenvalues and eigenvectors before attempting to determine them.

Analysis

Employing a Gaussian quadrature for the integral term of Eq. (1) over the range $-1 \leqq \mu \leqq 1$ gives the set of homogeneous differential equations

$$\frac{dI(\tau,x_i)}{d\tau} = \frac{-I(\tau,x_i)}{x_i} + \frac{W}{2x_i}\sum_{j=1}^{p} I(\tau,x_j)a_j, \qquad i = 1,\dots,p \tag{2}$$

where x_i are the quadrature points, a_j are the quadrature weight and p, which is even, is the order of the quadrature. The coefficient matrix of Eq. (2) is

$$B_{ij} = (Wa_j/2 - \delta_{ij})/x_i, \qquad i,j = 1,\dots,p \tag{3}$$

where δ_{ij} is the Kronecker delta. This matrix has exactly the same form whether the single Gaussian quadrature is employed over the interval $-1 \leqq \mu \leqq 1$ or if the double Gaussian quadrature is used separately in the regions $0 \leqq \mu \leqq 1$ and $-1 \leqq \mu \leqq 0$. For the latter case, the Gaussian quadrature of order $p/2$ is used twice, thus giving a $p \times p$ coefficient matrix of the form in Eq. (3). The quadrature points and weights are different for the two cases but in both instances they possess the common properties

$$x_k = -x_{p+1-k}, \qquad a_k = a_{p+1-k} \tag{4}$$

The eigenvalues of the coefficient matrix correspond to the values of λ which satisfy the determinant

$$|B_{ij} - \lambda\delta_{ij}| = |[Wa_j/2 - \delta_{ij}(1+x_i\lambda)]/x_i| = 0 \tag{5}$$

Now if $1/x_i$ is factored out from each row, Eq. (5) becomes

$$\left|\frac{Wa_j}{2} - \delta_{ij}(1+x_i\lambda)\right| \prod_{i=1}^{p}\left(\frac{1}{x_i}\right) = 0 \tag{6}$$

Since all of the x_i are finite and nonzero then the determinant in Eq. (6) must equal zero. One proceeds to simplify the determinant by 1) subtracting the last row from each of the previous rows, 2) factoring a $(-1-x_p\lambda)$ from the last column, and 3) subtracting from the last column each of the previous columns. Execution of these steps results in

$$(-1-x_p\lambda)\begin{vmatrix} -1-x_1\lambda & 0 & \cdots & 0 & x_1\lambda \\ 0 & -1-x_2\lambda & \cdots & 0 & x_2\lambda \\ \vdots & \vdots & & \vdots & \vdots \\ \vdots & \vdots & & -1-x_{p-1}\lambda & x_{p-1}\lambda \\ \frac{Wa_1}{2} & \frac{Wa_2}{2} & \cdots & \frac{Wa_{p-1}}{2} & \frac{Wa_p}{2(-1-x_p\lambda)} + 1 - \frac{W}{2}\sum_{i=1}^{p-1} a_i \end{vmatrix} = 0 \tag{7}$$

Recalling that

$$\sum_{i=1}^{p} a_i = 2$$

and therefore

$$\sum_{i=1}^{p-1} a_i = 2 - a_p$$

the element pp of Eq. (7) becomes

$$Wa_p/2(-1-x_p\lambda) + 1 - (W/2)(2-a_p) = 1 - W - (W/2)[a_p x_p\lambda/(-1-x_p\lambda)]$$

Substituting this relation for the element pp into Eq. (7) and expanding the determinant by the last column gives the result

$$(-1-x_p\lambda)\left[-\frac{W}{2}a_1x_1\lambda\frac{R}{F_1F_p} - \frac{W}{2}a_2x_2\lambda\frac{R}{F_2F_p} - \dots - \frac{W}{2}a_{p-1}x_{p-1}\lambda\frac{R}{F_{p-1}F_p} + \frac{R}{F_p}\left(1 - W - \frac{Wa_px_p\lambda}{2F_p}\right)\right] = 0 \tag{8}$$

where $F_i = -1 - x_i\lambda$ and

$$R = \prod_{i=1}^{p} F_i$$

Simplifying and gathering terms in Eq. (8) yields

$$-\frac{W}{2}\lambda R\sum_{i=1}^{p}\frac{a_ix_i}{F_i} + R(1-W) = 0 \tag{9}$$

with

$$\sum_{i=1}^{p}\frac{a_ix_i}{F_i} = \sum_{i=1}^{p/2}\frac{a_ix_i}{(-1-x_i\lambda)} + \sum_{i=1}^{p/2}\frac{a_{p+1-i}x_{p+1-i}}{(-1-x_{p+1-i}\lambda)} \tag{10}$$

Using the properties of Eq. (4), this expression becomes

$$\sum_{i=1}^{p}\frac{a_ix_i}{F_i} = \sum_{i=1}^{p/2}\frac{2a_ix_i^2\lambda}{(1-x_i^2\lambda^2)} \tag{11}$$

and also the expression for R becomes

$$R = \prod_{i=1}^{p/2}(-1-x_i\lambda)\prod_{i=1}^{p/2}(-1+x_i\lambda) = \prod_{i=1}^{p/2}(1-x_i^2\lambda^2) \tag{12}$$

The incorporation of Eqs. (11) and (12) into Eq. (9) gives

$$\left[\prod_{j=1}^{p/2}(1-x_j^2\lambda^2)\right]\left[W\sum_{i=1}^{p/2}\frac{a_ix_i^2\lambda^2}{1-x_i^2\lambda^2} - (1-W)\right] = 0 \tag{13}$$

The eigenvalues of Eq. (5) are the values of λ which satisfy Eq. (13). Equation (13) shows that the eigenvalues must either occur as complex conjugates, if the roots λ^2 are negative or complex, or as plus and minus pairs, if the roots λ^2 are positive.

Note that Eq. (13) is a function of λ^2. It will be shown that the roots λ^2 are positive or zero. Thus, the eigenvalues are real and occur as plus and minus pairs. When $W = 0$, the first factor of Eq. (13) must be zero, giving the p eigenvalues as $\lambda_j = \pm 1/x_j$, $j = 1,\dots,p/2$. If $W \neq 0$, the second factor must be zero. Setting the second factor equal to zero and simplifying, one finds the eigenvalues must satisfy the equation

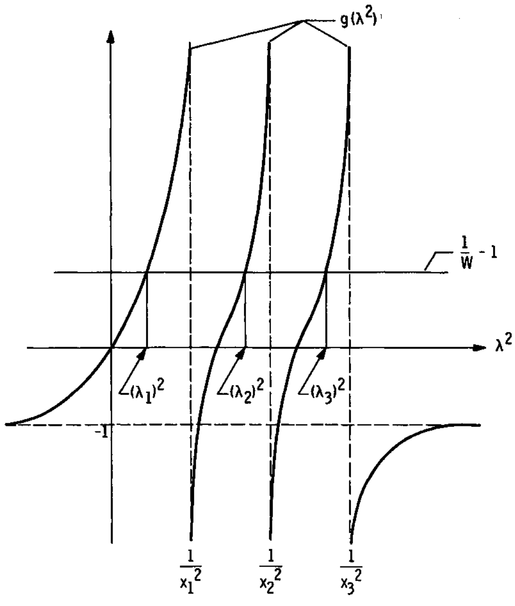

Fig. 1 Sketch illustrating graphical solution for the eigenvalues, $p = 6$.

$$g(\lambda^2) = \sum_{i=1}^{p/2} \frac{a_i x_i^2 \lambda^2}{(1 - x_i^2 \lambda^2)} = \frac{1}{W} - 1 \tag{14}$$

When $W = 1$, the right side is zero and it is seen $\lambda^2 = 0$ is a root. Thus, zero is an eigenvalue with a multiplicity of two. Plotting, simultaneously, $g(\lambda^2)$ and $1/W - 1$ vs λ^2 will give the solutions λ^2 where $g(\lambda^2)$ and $1/W - 1$ intersect. Figure 1 presents an illustrative plot for $p = 6$ but the analysis can be extended to any even value of p. Note that since $0 \leqq W \leqq 1$ then $0 \leqq 1/W - 1 \leqq \infty$, and therefore the values of $g(\lambda^2)$ where a solution is obtained must be in the region $0 \leqq g(\lambda^2) \leqq \infty$. It is seen from the graph that the values of λ^2 satisfying Eq. (14) must be positive or zero. Thus, all the eigenvalues must be real and must occur in plus and minus pairs except for $W = 1$ where two of the eigenvalues are equal to zero. Also, from Fig. 1 one can establish the bounds for the roots λ^2. For this example, $0 \leqq \lambda_1^2 \leqq 1/x_1^2 < \lambda_2^2 \leqq 1/x_2^2 < \lambda_3^2 \leqq 1/x_3^2$. Thus all the roots λ^2 have individual bounds. Using these bounds, the numerical solution for the roots of Eq. (14) is easily obtained. This is much simpler than using Danilevsky's method for finding the eigenvalues of a general matrix.

Having determined the nature of the eigenvalues and a simple technique for obtaining them, it is now necessary to compute the eigenvectors. Let v_{jk} be the jth component of the kth eigenvector. Then, the ith equation for the kth eigenvector is

$$\sum_{j=1}^{p} B_{ij} v_{jk} = \lambda_k v_{ik}, \qquad i = 1, \ldots, p$$

Substituting for B_{ij} from Eq. (3) and multiplying each equation by x_i results in

$$\frac{1}{2} W \sum_{j=1}^{p} a_j v_{jk} = (1 + \lambda_k x_i) v_{ik}, \qquad i = 1 \ldots, p \tag{15}$$

Since the eigenvalues occur in plus and minus pairs, let $\lambda_l = -\lambda_k$. Then, from Eq. (15)

$$\frac{1}{2} W \sum_{j=1}^{p} a_j v_{jl} = (1 + \lambda_l x_i) v_{il} = (1 - \lambda_k x_i) v_{il}, \qquad i = 1, \ldots, p$$

but by Eq. (4) one can write

$$\frac{1}{2} W \sum_{j=1}^{p} a_{p+1-j} v_{jl} = (1 + \lambda_k x_{p+1-i}) v_{il}, \qquad i = 1, \ldots, p \tag{16}$$

Let $i' = p + 1 - i$ and $j' = p + 1 - j$. Note there is no need to change the limits on the summation in Eq. (16) since the summation includes the same terms whether j' goes from p to 1 or 1 to p. Thus, Eq. (16) becomes

$$\frac{1}{2} W \sum_{j'=1}^{p} a_{j'} v_{(p+1-j')l} = (1 + \lambda_k x_{i'}) v_{(p+1-i')l}, \quad i' = 1, \ldots, p \tag{17}$$

From Eqs. (17) and (15) one concludes that

$$v_{(p+1-i)l} = v_{ik} \tag{18}$$

since both satisfy identical equations. This means it is only necessary to find the eigenvectors corresponding to the positive eigenvalues ($k = 1, \ldots, p/2$). The other $p/2$ eigenvectors, corresponding to the negative eigenvalues, are obtained by Eq. (18). Since it is only necessary to find $p/2$ eigenvectors, the work required in determining the eigenvectors has been reduced by one-half.

Now the system of equations represented by Eq. (15) will be solved for the eigenvectors in terms of the eigenvalues. Let λ_1 be the smallest positive eigenvalue, λ_2 the second smallest, etc., and

$$\lambda_i = -\lambda_{p+1-i}, \qquad i = 1, \ldots, p/2 \tag{19}$$

For the kth eigenvector, subtract the $(p+1-k)$th equation of Eq. (15) from all the other $p-1$ equations. Then, all the equations except the $(p+1-k)$th equation become

$$0 = (1 + \lambda_k x_i) v_{ik} - (1 + \lambda_k x_{p+1-k}) v_{(p+1-k)k}$$

so

$$v_{ik} = \frac{1 + \lambda_k x_{p+1-k}}{1 + \lambda_k x_i} v_{(p+1-k)k} = \frac{1 - \lambda_k x_k}{1 + \lambda_k x_i} v_{(p+1-k)k} \tag{20}$$

Notice that Eq. (20) is an identity for $i = p + 1 - k$. Thus, Eq. (20) holds for $i = 1, 2, \ldots, p$. Substituting Eq. (20) into Eq. (15) with $i = p + 1 - k$ and condensing the sum to $p/2$ terms by using Eq. (4) results in

$$\sum_{j=1}^{p/2} \frac{a_j}{1 - \lambda_k^2 x_j^2} = \frac{1}{W}$$

which is equivalent to Eq. (14); this is also the equation obtained in Ref. 5, although the method of derivation is entirely different. Thus the solution for the components of the kth eigenvector given by Eq. (20) satisfy the eigenvector equation for arbitrary $v_{(p+1-k)k}$ which will be chosen equal to one. From what was shown earlier about the nature of the eigenvalues, the denominator of Eq. (20) is never zero since only the $p/2$ positive eigenvalues are considered.

After the eigenvalues have been obtained, the eigenvectors are readily computed by Eq. (20) ($v_{(p+1-k)k} = 1$) and Eq. (18). Then the solution to the system of homogeneous equations, Eq. (2), is given by

$$I(\tau, x_i) = \sum_{j=1}^{p} c_j v_{ij} e^{\lambda_j \tau}, \qquad i = 1, \ldots, p \tag{21}$$

where c_j are the p integration constants. Substituting Eq. (20) into Eq. (21) and simplifying by using Eqs. (18) and (19), one obtains

$$I(\tau, x_i) = \sum_{j=1}^{p/2} \frac{1 - \lambda_j x_j}{1 - \lambda_j^2 x_i^2} [c_j (1 - \lambda_j x_i) e^{\lambda_j \tau} + c_{p+1-j} (1 + \lambda_j x_i) e^{-\lambda_j \tau}] \tag{22}$$

The c's are determined from the boundary conditions. For the special case of $W = 1$, the double eigenvalue $\lambda = 0$ causes Eq. (22) to have the special form

$$I(\tau, x_i) = c_1 + c_p \tau + \sum_{j=2}^{p/2} \frac{1 - \lambda_j x_j}{1 - \lambda_j^2 x_i^2} \times [c_j (1 - \lambda_j x_i) e^{\lambda_j \tau} + c_{p+1-j} (1 + \lambda_j x_i) e^{-\lambda_j \tau}] \tag{23}$$

Reference 5 also contains expressions equivalent to Eqs. (22) and (23) although the method of derivation is completely different.

Conclusions

In summary, it has been shown that for axisymmetric radiative transfer with isotropic scattering, the eigenvalues corresponding to the coefficient matrix are all real and occur in plus and minus pairs. For the matrix, Eq. (3), of any even order p, the eigenvalues have individual bounds which reduces the work required in determining them. Also, closed form expressions for the eigenvectors have been found in terms of the eigenvalues. Thus, once the eigenvalues are obtained from Eq. (14), the solution to the homogeneous system of equations is given directly by Eq. (22) or Eq. (23) ($W = 1.0$) without requiring separate calculation of the eigenvectors. Hence, the task of finding the eigenvalues and a solution of Eq. (2) has been accomplished. The method presented is simple and should significantly reduce the difficulties in obtaining solutions of the homogeneous system of equations given in Eq. (2).

References

[1] Hsia, H. M. and Love, T. J., "Radiative Heat Transfer Between Parallel Plates Separated by a Nonisothermal Medium with Anisotropic Scattering," *Journal of Heat Transfer*, Vol. 89, Ser. C, No. 3, Aug. 1967, pp. 197–204.

[2] Hottel, H. C., Sarofim, A. F., Evans, L. B., and Vasalos, I. A., "Radiative Transfer in Anisotropically Scattering Media: Allowance for Fresnel Reflection at the Boundaries," *Journal of Heat Transfer*, Vol. 90, Ser. C, No. 1, Feb. 1968, pp. 56–62.

[3] Merriam, R. L., "A Study of Radiative Characteristics of Condensed Gas Deposits on Cold Surfaces," Ph.D. thesis, 1968, Purdue Univ., Lafayette, Ind.

[4] Love, T. J., "An Investigation of Radiant Heat Transfer in Absorbing, Emitting, and Scattering Media," ARL 63-3, Jan. 1963, Aeronautical Research Labs., Office of Aerospace Research, Wright-Patterson Air Force Base, Ohio.

[5] Chandrasekhar, S., *Radiative Transfer*, Dover, New York, 1960, Chap. III.

Errata

Erratum: "Constitutive Equations for Bimodulus Elastic Materials"

FARHAD TABADDOR
The B.F. Goodrich Company, Akron, Ohio

[AIAA J. **10,** 516–518 (1972)]

THE following figure was inadvertently omitted from the April issue:

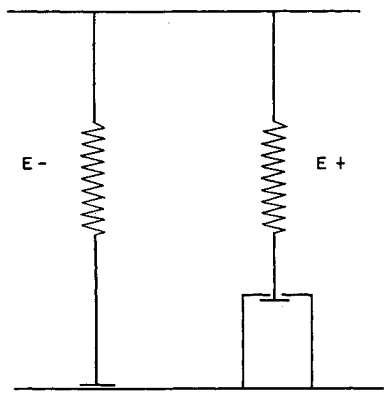

Fig. 1 One-dimensional model.